JOURNAL OF MATERIALS SCIENCE **38** (2003) 1835–1848

Review
Effect of anions on the textural and catalytic activity of titania

S. K. SAMANTARAY, K. M. PARIDA*
Regional Research Laboratory (CSIR), Bhubaneswar-751 013, Orissa, India
E-mail: kmparida@yahoo.com

An attempt has been made to review and studied the effect of ions (phosphate and sulfate) on titania samples. Surface area, average pore diameter and total pore volume increases however crystallite size decreases with increase in anion contents (both phosphate and sulfate case) up to 7.5 wt%, and thereafter decreases on further loading. TG-DTA and XRD patterns showed that phosphate stabilizes the anatase phase of TiO_2 up to 1173 K. FT-IR result showed that both phosphate and sulfate species strongly bound bidentately on TiO_2 support. Total acidity increases with increase in phosphate content up to 10.0 wt%, however, it increases up to 7.5 wt% in case of sulfated samples and thereafter decreases. Samples prepared at pH 3 and aqueous impregnation method exhibit higher acidity than the samples at pH 7 and solid-solid kneading method. Alkylation of benzene gives highest product (cumene) ≈70 mol% compared to others. Alkylation of aromatic compounds (benzene, toluene and chlorobenzene) with isopropanol is carried out in a fixed bed flow reactor over these catalysts as a function of benzene to isopropanol molar ratio, reaction temperature, percentage and source of sulfate ion.

1. Introduction

Metal oxides containing anionic species such as sulfate, phosphate, molybdates and tungstates, generally prepared by impregnation techniques, have recently received an increasing interest in the field of heterogeneous catalysis, because of their enhanced activity in typically acid catalysed reactions [1–3], and are considered as solid "superacids." This effect, particularly evident when titania and zirconia based powders are concerned, has been either attributed to the enhancement of the surface Lewis acid strength by inductive effect of the surface oxoanions [1, 2] or to the generation of very strong Brönsted acid sites [4]. Titania containing sulfates [1, 2], phosphates [5], and molybdates [6] are reported to behave as very strongly acidic materials. Oxide catalysts supported on titania are also deeply investigated in relation to their activity in selective catalytic oxidations and reduction of nitrogen oxides [7, 8]. The so called "solid phosphoric acid" (phosphoric acid impregnated on silica or kieselguhr) is a typical acidic heterogeneous catalyst widely used in industry for many years for olefin hydration to alcohols, proylene oligomerisation, alkylation and double-bond isomerisation of 1-butene and disproportionation of CCl_2F_2 [9–12].

Acid-base and redox properties are one of the more important types of surface chemical properties of metal oxide catalysts. From a catalytic point of view, TiO_2 possesses a unique type of surface involving both redox and acid-base sites. In addition to high thermal stability, its amphoteric character makes titania a promising catalytic material. The textural and acid-base properties of titania depend greatly on method of preparation, source and concentration of promoting elements and activation temperature [13–15].

In order to understand detail the generation of surface redox and acidity-basicity, we have prepared TiO_2 at different methods and impregnated by varying the source and concentration of anions. The samples are activated at different temperature and its activity and selectivity towards alcohol, cumene conversion reactions (probe reactions) and alkylation of aromatic compounds are reviewed.

2. Experimental

2.1. Materials and methods

Hydrated titania were prepared at pH 7 and 3 by adding 1:1 ammonia and water to the stirred aqueous solution of titanium tetrachloride, respectively. Obtained gels were filtered and washed repeatedly to remove Cl^- (negative $AgNO_3$ test), dried at 383 K for 10 h, powdered to 45–75 μm mess size and kept for anion impregnation.

2.2. Phosphate modified titania

A series of phosphated titania samples were prepared using $(NH_4)_3PO_4$ as a source of phosphate ions,

*Author to whom all correspondence should be addressed.

by solid-solid kneading method. The other series of phosphated titania samples were prepared by aqueous impregnation method using dilute H_3PO_4. The suspended mass was evaporated to dryness on a hot plate while stirring. After impregnation with phosphate the samples were dried in an air oven at 383 K and subsequent activated at 573, 773, 973, and 1173 K for activation in a muffle furnace. Then the samples were allowed to equilibrate with air, kept in an airtight bottle and stored in desiccator for further use.

2.3. Sulfate modified titania

A series of sulfated titania samples were prepared, using $(NH_4)_2SO_4$ as the source of sulfate ions, by solid-solid kneading method followed by slow heating at the rate of 283 K min^{-1} up to 773 K for 3 h. The other series of sulfated titania samples were prepared by aqueous impregnation method using dilute H_2SO_4. The suspended mass was evaporated to dryness on a hot plate while stirring, dried at 393 K and activated at 773 K for 3 h in a muffle furnace.

3. Characterisation

3.1. Determination of phosphate content

The concentration of phosphate ion in the above samples was measured using UV-visible spectrophotometer following the ascorbic acid reduction method [16].

3.2. Powder XRD study

The XRD patterns of all the samples were recorded on a Phillips (model: 1710) semiautomatic diffractometer using a Cu K_α radiation source and Ni filter in the range of $2\theta = 10$–80° at a scanning speed of 2°/min. The instrument was operated at 40 kV and 20 mA. The average crystallite size (L) of the particle was determined by XRD line broadening technique using a Scherrer equation,

$$L = 0.94\lambda/b\cos\theta \qquad (1)$$

where λ is the wavelength of X-ray used and b is the relative peak broadening, calculated as $b^2 = b^2_{\text{exp}} - b^2_{\text{ref}}$, where b_{exp} and b_{ref} are half-widths observed on a given sample and on a reference material, which is ideally crystalline, respectively.

3.3. FT-IR study

The IR spectra of unmodified and phosphate modified TiO_2 samples were recorded with a Perkin-Elmer (model-Paragon 500) FT-IR spectrometer in the range of 4000–400 cm^{-1} on pelletised with KBr phase (spectrophotometric grade). All the samples were degassed at 383 K in vacuum (1×10^{-4} Torr) before analysis. However, after 383 K evacuation in vacuum the samples were only retained the ligated water.

3.4. TG-DTA-DTG analysis

TG-DTA-DTG analyses of 383 K dried samples were carried out in dry air (50 cm^3/min) using a Shimadzu DT-40 thermal analyser in the range of 300 to 1273 K at a heating rate of 283 K/min.

3.5. Textural properties

Surface area (BET), average pore radius, and pore size distribution were determined by the N_2 adsorption-desorption method at liquid nitrogen temperature using quantasorb (Quantachrome, USA). Prior to adsorption-desorption measurements, the samples were degassed at 393 K at 10^{-4} Torr for 5 h.

3.6. Chemical surface properties

Surface acidity was determined by the spectrophotometric method [17] on the basis of irreversible adsorption of organic bases such as pyridine ($pK_b = 8.7$), morpholine ($pK_b = 5.67$), piperidine ($pK_b = 2.90$).

3.7. Catalytic activity

Catalytic activity of all the samples for dehydration/dehydrogenation of 2-propanol was studied using a fixed bed catalytic reactor (10 mm, i.d.) with on-line GC. Prior to reaction, catalysts were preheated in nitrogen atmosphere at 673 K for 1 h. Alcohol was supplied to the reactor by bubbling nitrogen gas through the alcohol container at 303 K. To avoid condensation of liquid

TABLE I Phosphate concentration and BET surface area of PO_4^{3-}/TiO_2 samples activated at different temperatures

		Concentration of phosphate (wt%)				
Sample no.	Sample code	383 K	573 K	773 K	973 K	1173 K
1	TiO_2	0(287)	0(131)	0(57)	0(13)	0(3)
2	2.5P/TiO_2	2.48(318)	2.59(192)	2.92(108)	2.90(32)	2.85(10)
3	5.0P/TiO_2	4.95(346)	5.20(262)	5.51(119)	5.55(51)	5.50(12)
4	7.5P/TiO_2	7.47(353)	7.62(273)	8.20(158)	8.22(57)	8.20(14)
5	10.0P/TiO_2	9.98(303)	10.18(258)	11.18(139)	11.20(34)	11.18(11)
6	7.5P/TiO_2(H*)	7.49(315)	7.51(252)	8.02(152)	8.03(32)	8.01(12)
7	10.0P/TiO_2(H*)	9.98(302)	10.06(244)	11.04(136)	11.03(31)	11.01(11)
8	7.5P/TiO_2(H)	7.46(471)	7.52(392)	8.04(173)	8.05(52)	8.03(18)
9	10.0P/TiO_2(H)	9.95(395)	10.08(356)	11.04(155)	11.05(48)	11.03(17)

Note: Data in parentheses denote the surface area (BET) in m^2/g. (H) and (H*) indicates H_3PO_4 impregnated samples prepared at pH 3 and 7, respectively.

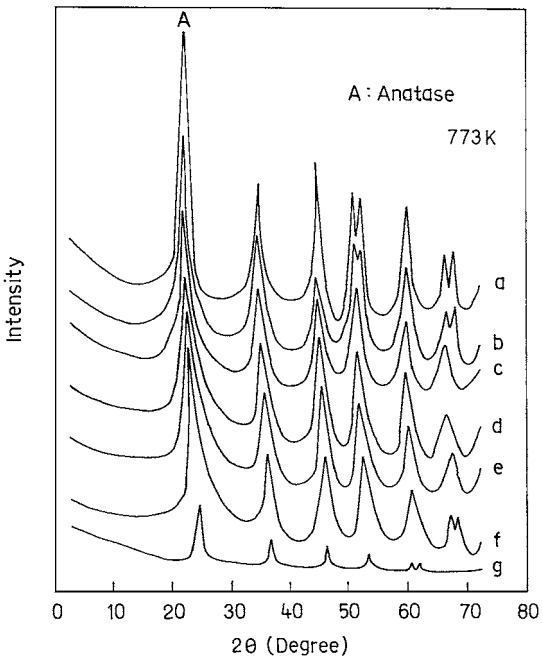

Figure 1 Powder XRD patterns of PO_4^{-3}/TiO_2 samples (a) TiO_2, (b) 2.5p/TiO_2, (c) 5.0P/TiO_2, (d) 7.5P/TiO_2, (e) 10.0P/TiO_2, (f) 10.0P/TiO_2 (H*) and (g) 7.5P/TiO_2 (H) activated at 773 K.

products in the apparatus, all the connections from the reactor to GC were heated at 393 K by heating tape. Reaction products were analysed by means of GC (CIC, India) in FID mode using Porapak Q columns.

The cumene cracking/dehydrogenation reaction was carried out in a micropulse reactor (Sigma, India) using nitrogen as the carrier gas in the temperature range of 673 to 873 K. Prior to the experiment, the catalyst was activated at 573 K for 1 h in nitrogen stream. The volume of one cumene pulse was maintained at 1 μl. All the products were analysed by GC using a 10 ft. SS column with 10% TCEP.

Alkylation of benzene and substituted benzenes with isopropanol were studied in a micropulse catalytic reactor (Sigma, India) with online GC. Prior to the reactions, all the catalysts were preheated in nitrogen atmosphere at 573 K for 1 h. The volume of each pulse (mixture of benzene or substituted benzenes and isopropanol) was maintained at 1 μl. Products were analysed by the gas chromatograph using 10-ft SS column with 10% TCEP.

4. Results and discussion

The phosphate concentration of the samples dried at 383 K and after being activated at 573, 773, 973 and 1173 K are shown in Table I. The concentration of phosphate ion in the samples are seen to increase with increased in activation temperature from 383 to 773 K and after that it remained almost constant till 1173 K. The reason for the initial increases in the wt% of phosphate with increases in the activation temperature of the samples can be assumed due to loss of water by dehydration.

The powder X-ray diffraction patterns of phosphate modified TiO_2 samples activated at 773, 573, 973 and 1173 K are shown in Figs 1, 2 and 3, respectively. It can be seen that samples prepared at pH 7 with very low or without any phosphate crystallised at 573 K while the samples prepared at pH 3 crystallised at higher temperatures ($\geq$773 K). From the XRD pattern (Fig. 2a, 973 K) it has been found that phosphate ion stabilise the anatase phase of titania. However, samples without any phosphate possesses mixture of anatase and rutile phases. It is also observed that (Fig. 3) when samples without phosphate activated at 1173 K possesses only rutile phase. However, sample with phosphate possesses mixture of anatase and rutile phases. There is no indication of titanium phosphate formation in any one of the samples. To develop a better

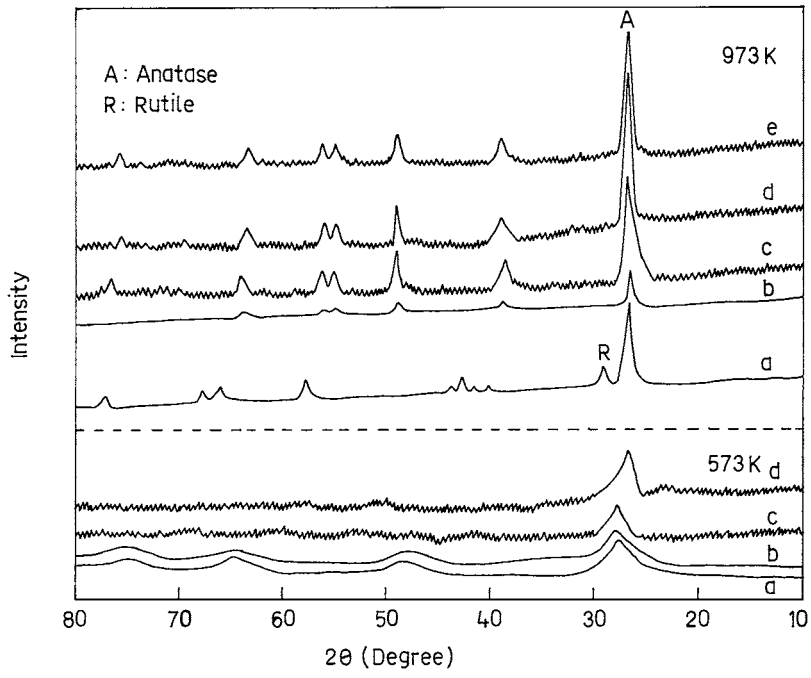

Figure 2 Powder XRD patterns of PO_4^{-3}/TiO_2 samples (a) TiO_2, (b) 2.5p/TiO_2, (c) 10.0P/TiO_2, (d) 10.0P/TiO_2 (H*) activated at 573 K and (a) TiO_2, (b) 2.5p/TiO_2, (c) 10.0P/TiO_2 (H), (d) 10.0P/TiO_2 (H*), (e) 10.0P/TiO_2 activated at 973 K.

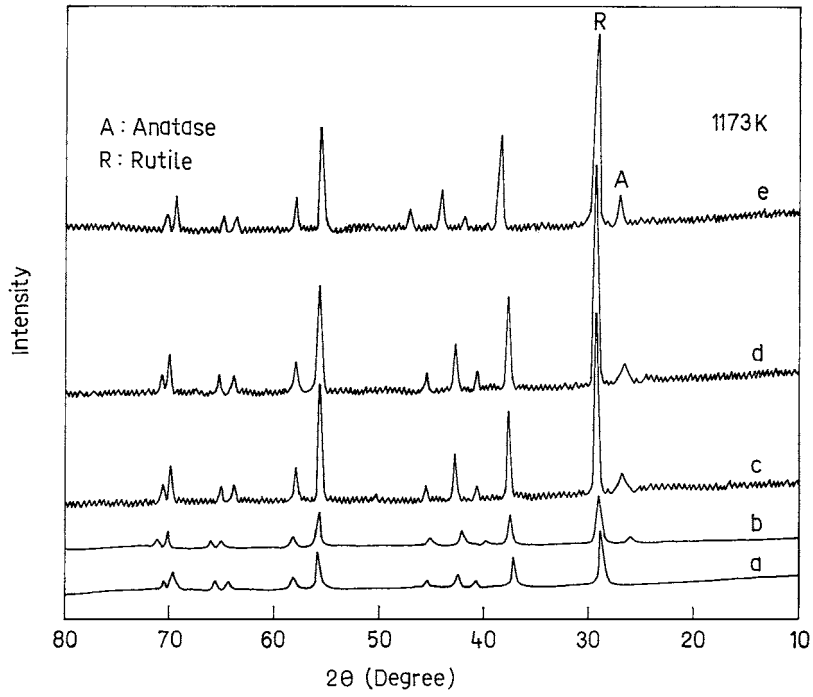

Figure 3 Powder XRD patterns of PO_4^{-3}/TiO_2 samples (a) TiO_2, (b) 2.5p/TiO_2, (c) 10.0P/TiO_2 (H), (d) 10.0P/TiO_2 (H*) and (e) 10.0P/TiO_2 activated at 1173 K.

understanding of formation and crystallisation in the presence of phosphate ion, the average crystallite size (L) perpendicular to the 210 plane was calculated from XRD patterns of pure titania, as well as phosphated titania. It is seen that the crystallite size of titania decreases with 2.5 wt% PO_4^{3-} loading and thereafter it remains the same. However, the effect is more pronounced with phosphoric acid as the source of phosphate compared to $(NH_4)_3PO_4$. This indicates that the crystallinity is more or less dependent on the presence of phosphate ion, but not on the source and percentage of phosphate loading. In addition to stabilising anatase TiO_2 crystallites, phosphate surface species inhibit TiO_2 crystallite sintering, leading to smaller crystallites than in pure TiO_2. The crystallite size decreases in the presence of phosphate ions as PO_4^{3-} species could possibly interact with TiO_2 network and, thus, hinder the growth of the particle. Even a very small amount of PO_4^{3-} species is responsible for this effect. Therefore, the change in phosphate concentration did not change on crystallite size further. Therefore, it is assumed that small amount of phosphate species is responsible for the lowering of crystallite size. From the Fig. 4 it is observed that crystallite size increases with increase in activation temperature from 573 to 773 K and thereafter it decreases. The former may be due to desorption of surface hydroxyl group from the TiO_2 network and the latter is due to the formation of rutile phase as well as inhibits sintering. This suggests that phosphate species strongly interacting with TiO_2 crystallites inhibit sintering even at high activation temperatures. This type of effect is also observed in PO_4^{3-} modified FeO(OH) [18], WO_3 modified ZrO_2 [19] and TiO_2 [20].

SO_4^{2-}/TiO_2 samples activated at 773 K exhibit only anatase phase XRD pattern (Fig. 5) irrespective of the source and % of loading of sulfate ion. There is no

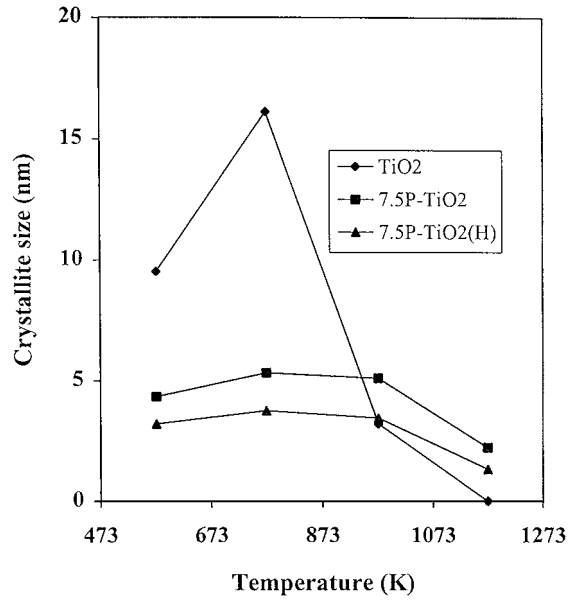

Figure 4 Average crystallite of samples activated at different temperatures.

indication of formation of titanium sulfate in any one of the samples; even in 10 wt% SO_4^{2-} impregnation. The average crystallite size (L) of pure titania as well as sulfate modified titania and is represented in Table II. It shows the similar results as PO_4^{3-}/TiO_2 samples.

The IR absorption spectra of the unmodified and phosphated titania samples activated at different temperatures are shown in Fig. 6. The bands at 3430 and 1630 cm^{-1}, possessed by all the samples even after activated at 773 K, correspond to the specifically for OH stretching and bending vibrations, respectively. This absorption band assigned to the strongly H-bonded H—O—H species may be due to the residual surface hydroxyl groups/ligated H_2O in the samples. Infrared

TABLE II Textural parameters of sulfated titania

Sample code	SO_4^{2-}(wt%)	S_{BET} (m^2/g)	Total pore volume (cm^3/g)	Average pore diameter (A°)	Crystallite size (nm)
TiO_2	0	57.0	0.09	67.00	16.13
2.5S/TiO_2	2.5	73.9	0.13	61.78	7.08
5.0S/TiO_2	5.0	74.4	0.18	65.56	–
7.5S/TiO_2	7.5	94.5	0.22	74.56	6.8
10.0S/TiO_2	10.0	84.6	0.20	62.12	–
2.5S/TiO_2(H*)	2.5	75.2	0.14	64.10	–
5.0S/TiO_2(H*)	5.0	81.2	0.20	70.20	–
7.5S/TiO_2(H*)	7.5	108.5	0.23	80.92	6.5
10.0S/TiO_2(H*)	10.0	91.0	0.21	72.20	–

Note: (H*) indicates H_2SO_4 impregnated samples prepared at pH 7.

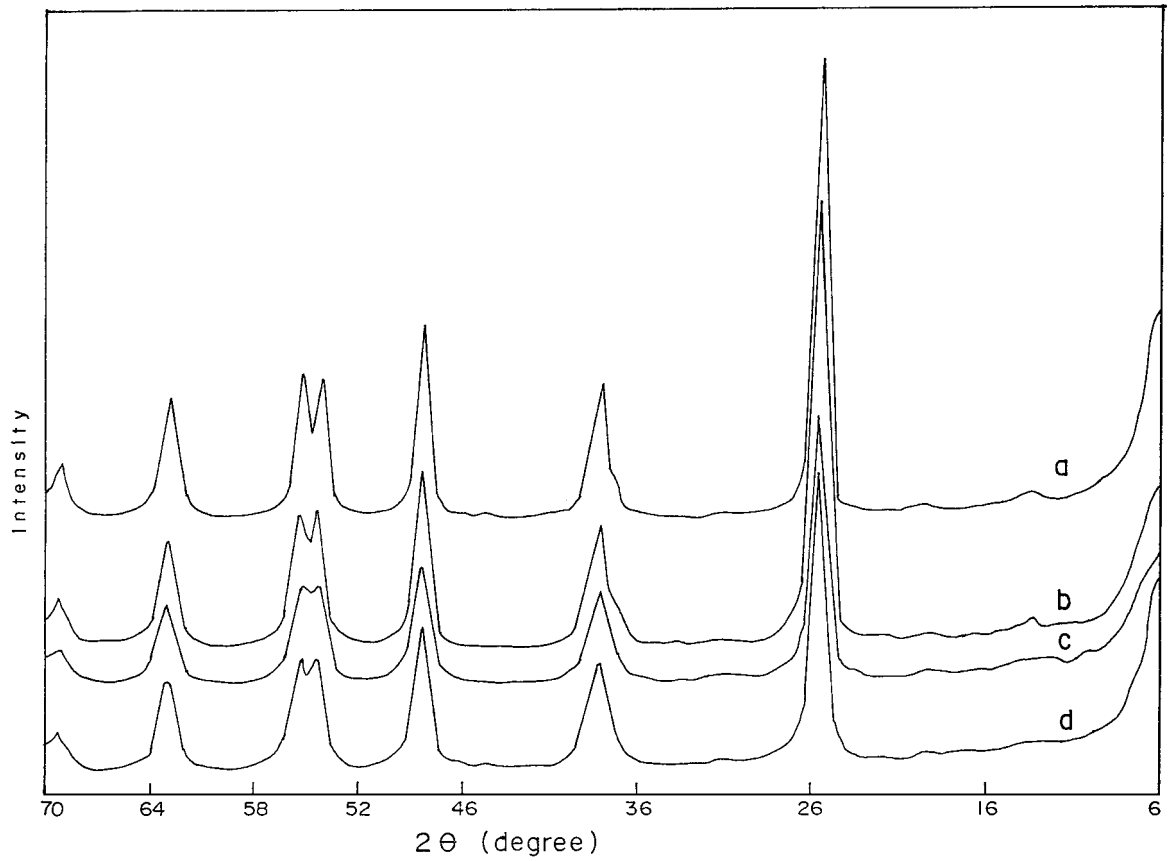

Figure 5 Powder XRD patterns of SO_4^{-2}/TiO_2 samples (a) TiO_2, (b) 2.5S/TiO_2, (c) 7.5S/TiO_2, and (d) 7.5S/TiO_2 (H*) activated at 773 K.

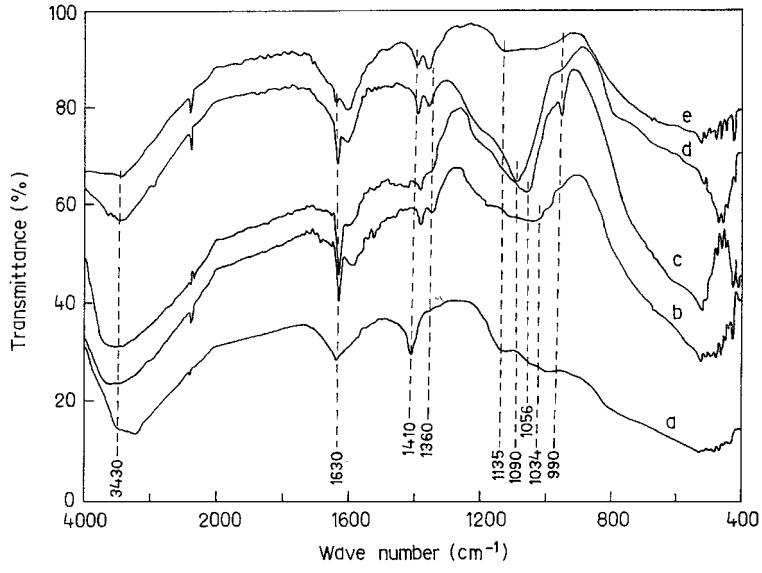

Figure 6 FT-IR spectra of (a) 10.0P/TiO_2 (H), 773 K and (b), (c), (d), (e) are 10.0P/TiO_2 samples activated at 573, 773, 973 and 1173 K, respectively.

spectra of phosphated metal oxide generally show a strong sharp absorption band at 1300–1450 cm^{-1} and broad bands at 950–1150 cm^{-1}. The 1300–1450 cm^{-1}peak is the stretching frequency of P—O bonds whose order is close to two (P═O, phosphoryl groups) and the 950–1150 cm^{-1} peaks are the characteristic frequencies of PO_4^{3-}. The broad bands at 950–1150 cm^{-1} resulted from the lowering of the symmetry in the free PO_4^{3-} (Td point group). The PO_4^{3-} is bound to the titania surface, the symmetry can be lower to either C_{3V} or C_{2V} [21]. Here, the band that split into 3 peaks (1056, 1034, 990 cm^{-1}) were assigned to the bidentately bound phosphate ion (C_{2V} point group). These three bands somewhat shifted to higher wave number (1090 and 1135 cm^{-1}) when the sample is activated above 973 K and sample prepared at pH 3. This agrees with the position of such a fundamental band, as has been directly observed in the case of phosphated zirconia [22] and alumina [23]. The above results give several indications of the structure of the phosphate species supported on the titania supports. Based on the main IR features discussed above the surface structures are reported in Scheme-I.

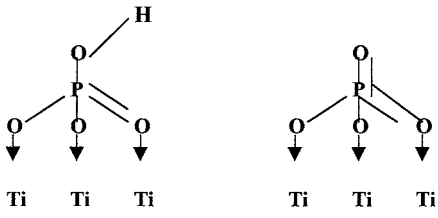

$\bar{\nu}$P (OH) = 950-1150 cm^{-1} (Covalent bond)

$\bar{\nu}$PO = 1300-1450 cm^{-1} (Coordinated bond)

Scheme 1

Infrared spectra of sulfated metal oxides generally show a strong absorption band at 1381 cm^{-1} and broad bands at 1250–1100 cm^{-1} (Fig. 7). The 1381 cm^{-1} peak is the stretching frequency of S═O and the 1250–1100 cm^{-1} peaks are the characteristic frequencies of SO_4^{2-}. The broad bands at 1250–1100 cm^{-1} results from lowering of the symmetry in the free SO_4^{2-} (Td point group). When SO_4^{2-} is bound to the titania surface, the symmetry can be lowered to either C_{3V} or C_{2V} [21]. Here the band split into three peaks (1221, 1119, 1026 cm^{-1}) were assigned to the bidentately bound sulfate ion (C_{2V} point group).

From the TG-DTA analysis it is observed that the samples undergo consistent weight loss below 573 K, due to desorption of water molecules. Successively a slight continuous weight loss is observed until 873 K for phosphated sample and until 973 K for unmodified sample. The absence of relevant weight loss above 873 K in case of phosphated samples would also indicate that phosphate ion is rather strongly bonded to the support and does not desorb nor evaporate on heating. Desorption of water correspond to endothermic peak in the DTA curves (Fig. 8). The exothermic peak observed very clearly for phosphate modified titania and, to a lower extent, for unmodified titania in the reason near 1173 K without any corresponding weight loss is due to solid-state transformations (anatase to rutile transformation). This result is further supported by XRD analysis. Its position at so high a temperature that agrees with the inhibiting effect of phosphate species on the anatase to rutile transformation already reported [24].

The TG-DTG curves of the sulfate modified samples prepared from $(NH_4)_2SO_4$ and H_2SO_4 obtained in air reported in Fig. 9a and b, respectively. All the

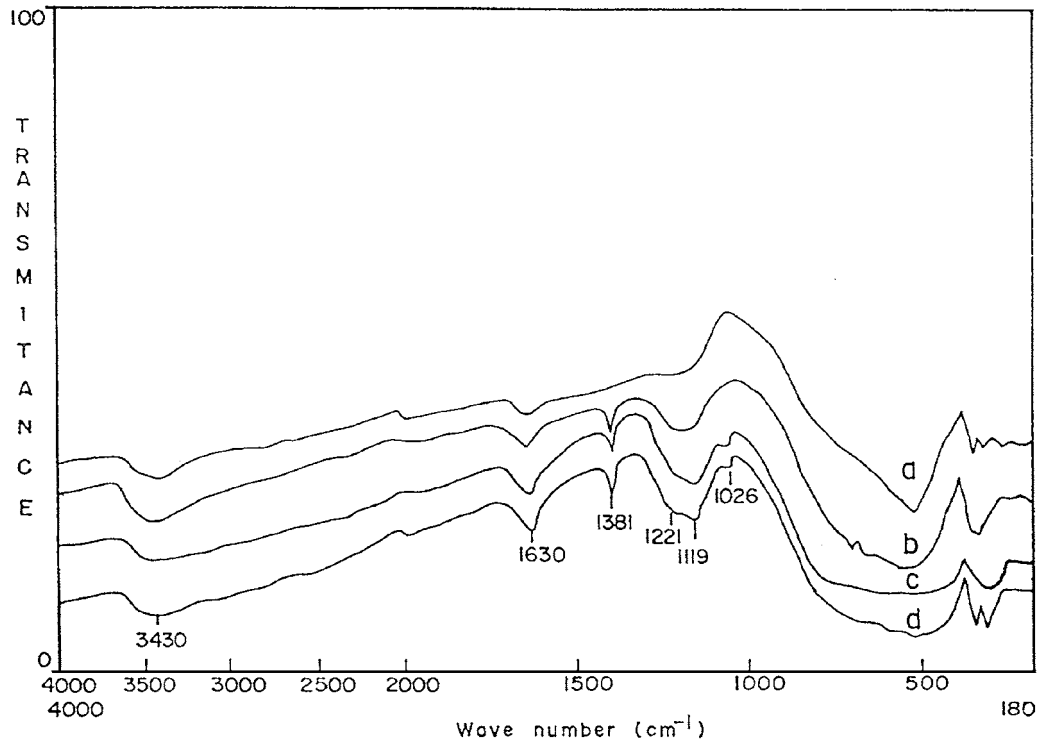

Figure 7 FT-IR spectra of (a) TiO_2, (b) 2.5S/TiO_2, (c) 7.5S/TiO_2, and (d) 7.5S/TiO_2 (H^*) activated at 773 K.

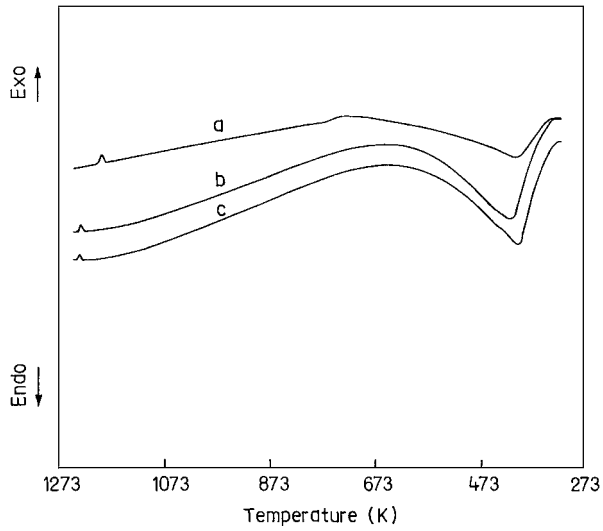

Figure 8 Differential thermal analysis of (a) TiO_2, (b) 10.0P/TiO_2 and (c) 10.0P/TiO_2 (H^*) samples.

samples undergo consistent weight loss below 573 K which was most likely due to the desorption of molecular water from the sample. At higher temperatures there were two modes of weight loss in case of sulfated sample. The first (termed mode I) had a peak at 773–873 K and had a maximum around 850 K. The second (mode II) had a peak between 873–1073 K with a maximum at ca. 950 K. As was reported earlier [25] the first mode corresponds to the sulfate transition from low temperature (LT) to high temperature (HT) species mentioned above, while the second mode is due to the sulfate decomposition. Foe $7.5SO_4^{2-}/TiO_2$ (H^*) sample prepared from H_2SO_4, the transition as well as decomposition took place slightly higher activation temperature than $7.5SO_4^{2-}/TiO_2$ sample prepared from $(NH_4)_2SO_4$.

The values in parentheses (Table I) show the BET surface area of the samples in square meters per gram. With the increase in phosphate content from 0 to 7.5 wt%, the surface area of the material are increases from 287

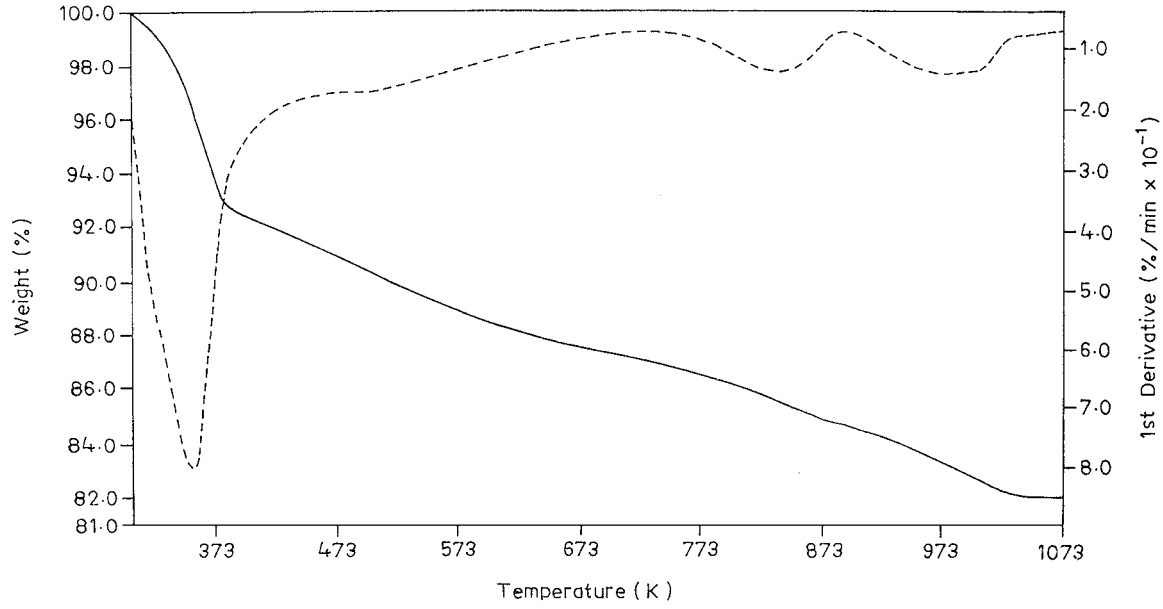

Figure 9a TG-DTG curves of the sulfate modified samples prepared from $(NH_4)_2SO_4$.

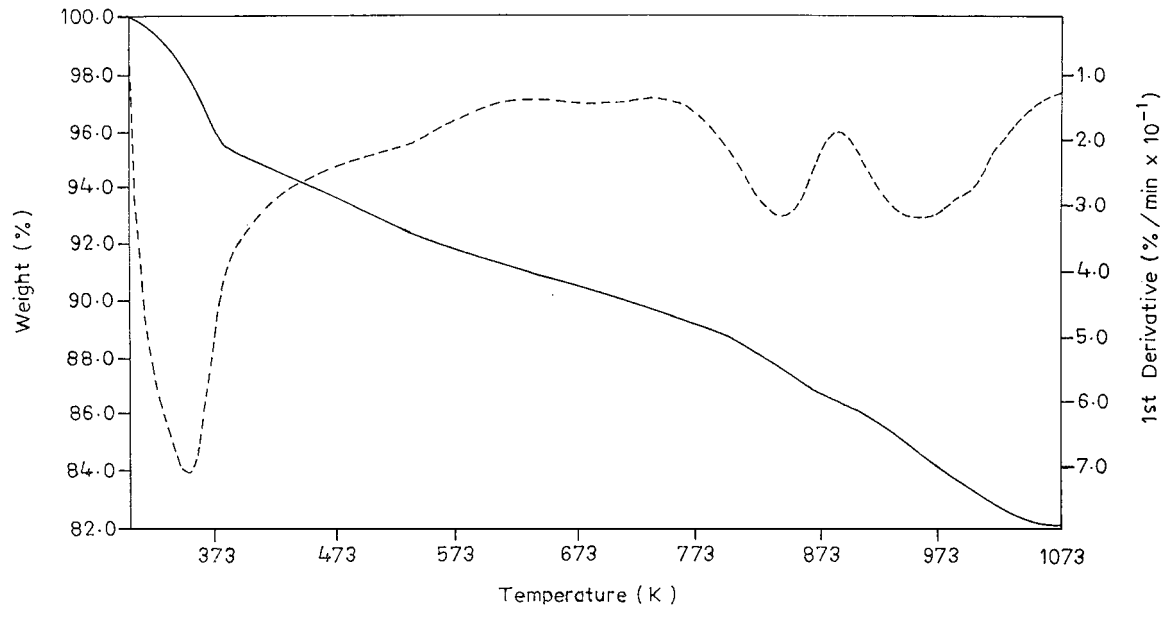

Figure 9b TG-DTG curves of the sulfate modified samples prepared from H_2SO_4.

to 353 m^2/g in case of 383 K dried samples. However, at 10.0 wt% PO_4^{3-}, the surface area is decreases to 303 m^2/g. The same trend are observed irrespective of the source of phosphate ion, method of preparation and for samples activated at different temperatures, i.e., 573, 773, 973, and 1173 K. This implies that the presence of PO_4^{3-} ions plays a role in making the material porous. However, when the phosphate content increases beyond 7.5 wt%, pore blocking takes place due to the presence of an excess amount of phosphates. This type of observation was also noted in case of phosphated zirconia [26]. With increase in activation temperature the surface area decreases gradually. This might be due to the inter-particle agglomeration or due to collapse of very fine/narrow pores. It is also observed that the sample prepared at pH 3 has higher surface area compared to the sample prepared at pH 7.

The nitrogen adsorption-desorption isotherm of some representative samples are shown in Figs 10 and 11. All of the curves are nearly same type and can be assigned as type IV or II in the BDDT classification [27]. From the shape of the curves it can be predicted that samples activated at 1173 K consists of mainly mesopores. However, samples with varying source of phosphate ion and method of preparation are micro-mesopores. A similar observation can also be drawn from the pore size distribution curves (Fig. 12a and b) calculated by BJH equation [28]. So due to the microporosity, samples prepared at pH 3 show a very high surface area. The t-plots (Fig. 13) of sample activated at different temperatures (up to 973 K), varying source of phosphate ion and method of preparation show a downward deviation except for sample activated at 1173 K. The downward deviation reveals that these samples contain predominantly micropores along with some mesopores, whereas an upward deviation indicates the presence of mesopores. The upward deviation pore samples activated at 1173 K may be explained by an enhanced adsorption due to capillary condensation into mesopores 4–10 nm in diameter [29].

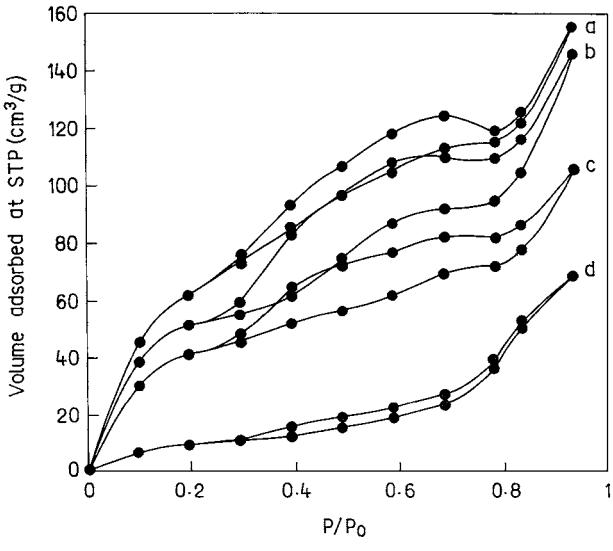

Figure 10 Nitrogen adsorption-desorption isotherms of (a), (b), (c) and (d) 7.5P/TiO_2 samples activated at 573, 773, 973 and 1173 K, respectively.

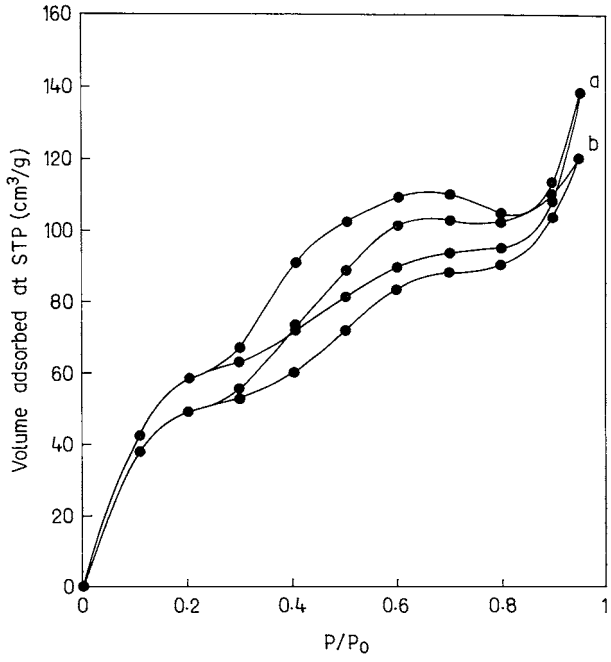

Figure 11 Nitrogen adsorption-desorption isotherms of (a) 7.5P/TiO_2 (H^*) and (b) 7.5P/TiO_2 (H) samples activated 773 K.

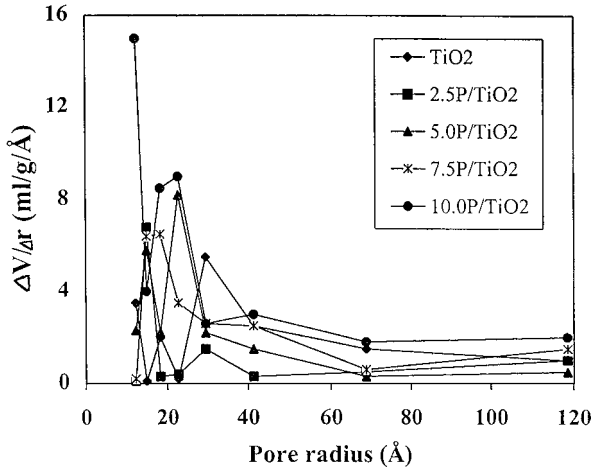

(a)

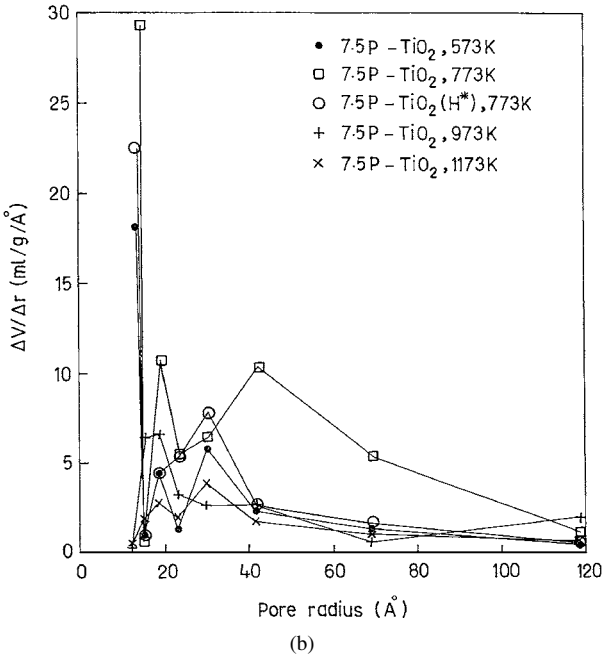

(b)

Figure 12 Distribution of pores as a function of pore radius.

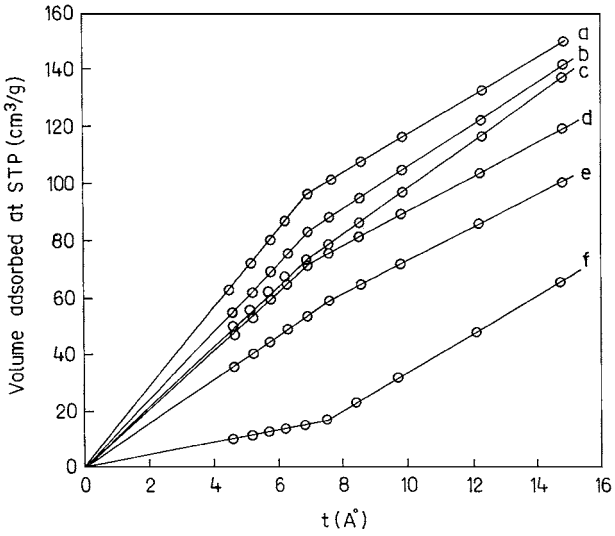

Figure 13 t-plots for (a) 7.5P/TiO_2, 573 K; (b) 7.5P/TiO_2, 773 K; (c) 7.5P/TiO_2 (H*), 773 K; (d) 7.5P/TiO_2 (H), 773 K; (e) 7.5P/TiO_2, 973 K and (f) 7.5P/TiO_2, 1173 K samples.

It is observed that increase in sulfate loading increases the surface area up to the sulfate loading of 7.5 wt%. Further increase in sulfate loading to 10 wt% resulted in a decrease in surface area (Table II). The trend remains same irrespective of the source of sulfate ion. Similar trend is also maintained in case of the pore volume for both the series of materials. Therefore, the presence of low amount of sulfate ion ($\leq$7.5 wt%) may be responsible in the formation of porous network. It has been shown [30, 31] that, in sulfated metal oxides some of the hydroxyl bridges originally present in dried unactivated and unsulfated titania replace by sulfate ions. On activation, the formation of oxy bonds takes place and results in changes in the Ti—O—Ti bond strength due to attachment of the sulfate bridges. Thus the changes in the Ti—O—Ti bond strength may be responsible for the formation of porous network. Consequently, the increase in surface area with an increase in sulfate loading up to 7.5 wt% appears is due to the stabilizing effect of the sulfate ions. However, the plugging of more pores may have occurred with higher sulfate loading resulting in a reduction of total pore volume to some extent and also decrease in surface area [30].

Average pore diameter is found to be in the same range irrespective of sulfate concentration and source of sulfate ion. This is also supported by the mesopore size distribution curve (Fig. 14) calculated by BJH equation [28].

It is seen from Table III that the Hammett acidity function of 7.5PO_4^{3-}/TiO_2 is ≥ -13.16 and

TABLE III Acid strength of phosphated and sulfated titania samples activated at 773 K

	pK_a value of indicators					
Sample code	−3.0	−5.6	−8.2	−12.4	−13.16	−14.52
TiO_2	+	−	−	−	−	−
2.5P/TiO_2	+	+	+	+	±	−
7.5P/TiO_2	+	+	+	+	±	−
7.5P/TiO_2 (H)	+	+	+	+	+	−
7.5P/TiO_2 (H*)	+	+	+	+	+	−
7.5S/TiO_2	+	+	+	+	+	+
7.5S/TiO_2 (H*)	+	+	+	+	+	+

Note: (H) and (H*) indicates H_3PO_4 or H_2SO_4 impregnated samples prepared at pH 3 and 7, respectively.

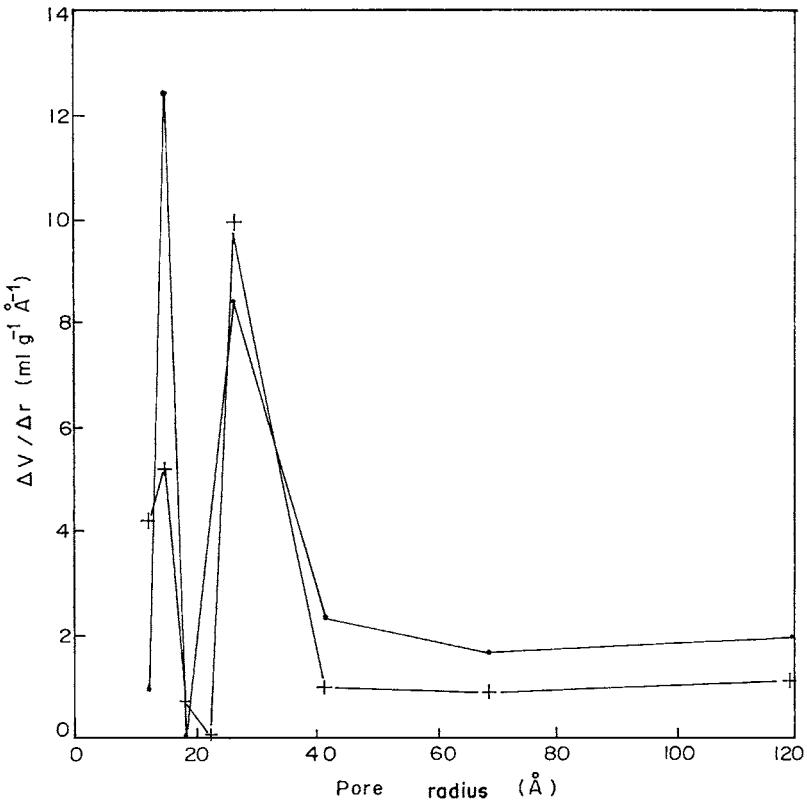

Figure 14 Distribution of pores as a function of pore radius of (•) 7.5S/TiO_2, (+) 7.5S/TiO_2 (H*).

$7.5SO_4^{2-}/TiO_2$ is ≥ -14.52, where as for TiO_2 it is ≥ -3.0. These results mean that the weak acid sites of unmodified titania are converted into strong acid sites by means of phosphate as well as sulfate ion modification. Acid stronger than $H_o = -11.93$, which corresponds to the acid strength of 100% H_2SO_4, are known as super acids [32] and the $7.5PO_4^{3-}/TiO_2$ and $7.5SO_4^{2-}/TiO_2$ acts as solid super acid catalysts. The increase in acid strength in the modified catalyst is attributed to the double bond nature of X=O (X is either P or S), which strengthens the acid sites by the inductive effect [33].

The total acidity measured by the adsorption of piperidine, strong acid sites by pyridine, and moderate acid sites by morpholine all gradually increased with increase in phosphate wt% up to a value of 10.0 (Table IV). This indicates that all types of acid sites are present in phosphated titania. It is observed that phosphated samples prepared using phosphoric acid as the source of phosphate ion exhibit higher acidity compared to the sample prepared using ammonium phosphate. It is also observed that PO_4^{3-}/TiO_2 samples prepared at pH 3 exhibit higher acidity compared to the PO_4^{3-}/TiO_2 samples prepared at pH 7. It is reasonable to assume that during the preparation procedure, the aqueous phosphoric acid protonates all types of titania hydroxyls by an acid-base reaction. However, phosphate of ammonium phosphate by solid-solid leading method undergoes interaction with all types of basic hydroxyls to a smaller extent resulting in less acidity compared to the phosphate of phosphoric acid by aqueous impregnation method. Similar observations have been reported earlier in case of SO_4^{2-} [34] and PO_4^{3-} [35] on alumina. It can be seen from Table IV that with increase in activation temperature from 573 to 1173 K, the acid sites are found decrease, due to the loss of bonded hydroxyl groups.

Similarly, the total acid sites, strong acid sites, and moderate acid sites, gradually increases with increase in sulfate loading of up to 7.5 wt% and thereafter decreases on further addition (Table V). This indicates that all types of acid sites are present in SO_4^{2-}/TiO_2. The initial increase in surface acidity with increase in sulfate loading up to 7.5 wt% may be due to sulfate monolayer formation. The decrease in the surface acidity at high sulfate concentrations is probable due to the formation of polysulfate, which decreased the number of Brönsted sites and consequently that of total acid sites [36]. It is observed that sulfated samples prepared using sulfuric acid exhibit higher acidity compared to the samples prepared using $(NH_4)_2SO_4$. It is reasonable to assume that during the preparation procedure, the aqueous sulfuric acid protonates all types of titania hydroxyls by an acid-base reaction (Scheme-II):

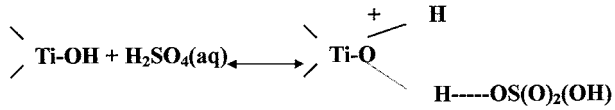

Scheme 2

However, sulfate of ammonium sulfate by solid-solid kneading method undergoes interaction with all types of basic hydroxyls to a smaller extent resulting in less acidity compared to sulfate of sulfuric acid by aqueous impregnation method.

The 2-propanol conversion produces both propene and acetone as major products, while diisopropyl ether is found as a minor product. In unmodified titania acetone selectivity is more than propene selectivity. However, with the increase in phosphate contents in the sample, propene selectivity increases (Table VI). On all the catalysts higher acetone selectivity is found at low temperature. With the increase in propene formation,

TABLE V Acid sites of sulfated titania samples

Sample	SO_4^{2-} (wt%)	Acidity (μmol/g) PP ($pK_a = 11.1$)	MOR ($pK_a = 8.33$)	Py ($pK_a = 5.3$)
TiO_2	0	220	182	120
2.5S/TiO_2	2.5	382	287	225
5.0S/TiO_2	5.0	485	322	233
7.5S/TiO_2	7.5	622	425	280
10.0S/TiO_2	10	443	341	205
7.5S/TiO_2 (H*)	7.5	681	522	303
10.0S/TiO_2 (H*)	10.0	455	345	221

Note: (H*) indicates H_2SO_4 impregnated samples prepared at pH 7.

TABLE IV Surface acidity of the PO_4^{3-}/TiO_2 samples activated at different temperatures

Sample no.	Surface acid sites (μmol/g) Piperidine ($pK_b = 2.90$) (a)	(b)	(c)	(d)	Morpholine ($pK_b = 5.67$) (a)	(b)	(c)	(d)	Pyridine ($pK_b = 8.70$) (a)	(b)	(c)	(d)
1	1012	260	210	102	697	143	117	41	233	100	46	7
2	1088	360	305	171	769	280	257	128	319	202	88	12
3	1163	401	390	241	903	325	271	215	374	220	109	18
4	1281	445	408	295	914	340	315	245	400	264	129	19
5	1331	497	482	305	992	361	383	266	444	299	182	21
6	1229	466	425	317	1002	351	403	367	431	273	172	20
7	1458	602	515	325	1109	445	421	393	456	377	255	25
8	1598	944	–	–	1170	665	–	–	505	407	–	–
9	1602	964	–	–	1485	727	–	–	512	503	–	–

Note: (a) 573 K, (b) 773 K, (c) 973 K, (d) 1173 K activation.

TABLE VI Conversion (mol%) of 2-propanol over PO_4^{3-}/TiO_2 using nitrogen as carrier

	Reaction temperature											
	393 K				433 K				473 K			
Sample no.	(a)	(b)	(c)	(d)	(a)	(b)	(c)	(d)	(a)	(b)	(c)	(d)
1	2(0)	0(0)	0(0)	0(0)	4(0)	0(0)	0(0)	0(0)	8(96)	2(90)	1(76)	0(0)
2	7(100)	4(98)	2(94)	1(80)	10(96)	7(90)	6(82)	3(70)	18(82)	12(78)	10(60)	6(42)
3	6(94)	3(92)	2(90)	1(68)	8(80)	6(72)	5(60)	3(52)	15(68)	10(60)	6(46)	4(32)
4	5(58)	2(52)	1(48)	0(0)	7(28)	5(24)	5(18)	2(12)	13(10)	9(6)	4(4)	3(0)
5	5(28)	1(18)	1(10)	0(0)	6(14)	4(10)	3(6)	1(2)	10(0)	7(0)	3(0)	1(0)
6	6(12)	2(14)	1(6)	0(0)	9(10)	5(8)	4(0)	2(0)	14(0)	9(0)	5(0)	4(0)
7	8(8)	2(12)	1(4)	0(0)	12(6)	5(4)	4(0)	2(0)	18(0)	10(0)	8(0)	6(0)
8	7(4)	3(10)	2(0)	1(0)	15(0)	7(2)	6(0)	4(0)	23(0)	12(0)	10(0)	8(0)
9	10(0)	3(6)	2(0)	1(0)	19(0)	10(0)	8(0)	6(0)	28(0)	13(0)	12(0)	10(0)

Note: (a) 573 K, (b) 773 K, (c) 973 K, (d) 1173 K activation. Values in parentheses represent percentage selectivity to dehydrogenation product.

acetone selectivity drastically decreases. This may be due to the poisoning of the basic sites by the water molecules formed by a dehydration process.

In the case of unmodified titania, acetone formation started at 453 K while on the 2.5 wt% phosphated sample the same reaction starts at 393 K. This drastic decrease in the reaction temperature indicates that the phosphate molecule plays some role in the dehydrogenation process. However, with the increase in phosphate content, acetone selectivity decreases. Therefore, dehydrogenation takes place on the basic sites present in the titania surface. With the increase in the phosphate content these site are poisoned by the phosphate molecule [37], thus decreasing the dehydrogenation selectivity. However, the small amount of phosphate probably acts as a promoter for the dehydrogenation reaction, thus decreasing the reaction temperature. Among all the samples 10.0P-TiO_2 (H*) show higher propene selectivity. The 2-propanol conversion is highest on 10.0P-TiO_2 (H*), whereas acetone selectivity is more in the case of 10.0P-TiO_2, though both the samples contain the same amount of phosphate. Therefore, it can be interpreted that the surface acid-base sites can be control by varying the method of preparation.

Among 573, 773, 973, and 1173 K activation, 573 K activated samples have shown maximum 2-propanol conversion activity followed by 773, 973 and 1173 K activated samples. The selectivity to dehydrogenation product decreased as the activation temperature increased. This is quite similar to surface acidity of the samples which has followed the same trend. From this we can say that the total conversion of 2-propanol is a function of total acidity.

With increase in sulfate content up to 7.5 wt% in the sample, propene selectivity increases, thereafter decreases. Phosphate titania samples also behaved similarly. The only difference is that sulfated titania gives more conversion at low temperature than phosphated titania samples (Table VII). That means sulfated samples have more number of acid/basic sites as well as strength than phosphated titania samples. Among all the samples $7.5SO_4^{2-}/TiO_2$ (H*) shows higher propene selectivity. The 2-propanol conversion is highest on $7.5SO_4^{2-}/TiO_2$ (H*), whereas acetone selectivity is more in the case of $7.5SO_4^{2-}/TiO_2$, though both the samples contain the same amount of sulfate.

TABLE VII Conversion (mol%) of 2-propanol over SO_4^{2-}/TiO_2 activated at 773 K using nitrogen as carrier

	Reaction temperature (K)				
Catalysts	453	493	533	573	613
TiO_2	0	3.0(96)	16.4(82)	30.2(65)	50.3(55)
2.5S/TiO_2	1.2(100)	5.8(92)	19.3(79)	32.8(62)	71.5(30)
5.0S/TiO_2	2.5(91)	7.3(80)	22.2(68)	33.2(53)	73.3(25)
7.5S/TiO_2	5.3(75)	10.0(62)	33.5(51)	50.4(43)	98.6(21)
10.0S/TiO_2	4.4(62)	8.2(50)	30.0(42)	47.5(33)	90.2(15)
7.5S/TiO_2 (H*)	6.6(52)	12.3(42)	35.2(30)	56.5(27)	99.1(12)
10.0S/TiO_2 (H*)	4.8(43)	9.6(37)	32.3(22)	48.2(12)	92.8(3)

Note: (H*) indicates H_2SO_4 impregnated samples prepared at pH 7. Values in parentheses represent percentage selectivity to dehydrogenation product.

Table VIII presents the results of the cumene conversion reaction. In the conversion of cumene, two types of reactions occur, i.e., cracking to benzene and propene and dehydrogenation to α-methyl styrene. The table includes both the percentage of total conversion and the benzene to α-methyl styrene ratio (value inside the parentheses). From the table it is found that with the increase in the phosphate content, total cumene conversion increases. In a particular sample (pH 3) prepared from H_3PO_4 exhibit higher conversion than both the samples (pH 7) prepared from H_3PO_4 and $(NH_4)_3PO_4$, though these samples contain same amount of phosphate (10.0 wt%). From the benzene to α-methyl styrene ratio it is well marked that the benzene selectivity is higher at low temperature conversion. With the increase in reaction temperature, α-methyl styrene selectivity increases. In the case of unmodified titania α-methyl styrene selectivity is more than the benzene selectivity. However, with the increase in phosphate content benzene selectivity increases at all reaction temperature. It is known that cracking proceeds over Brönsted acid sites whereas dehydrogenation occurs on Lewis acid sites. Thus, it can be concluded that the unmodified titania mostly contains Lewis acid sites. With the increase in phosphate impregnation the number of Lewis acid sites decreases, thus decreasing the α-methyl styrene selectivity.

TABLE VIII Results of cumene cracking/dehydrogenation (mol%) over PO_4^{3-}/TiO_2

	Reaction temperature								
	573 K			673 K			773 K		
Sample no.	(a)	(b)	(c)	(a)	(b)	(c)	(a)	(b)	(c)
1	1.3(3.3)	0(0)	0(0)	4.2(5)	3.5(0.16)	0(0)	35(5.3)	30.7(0.33)	10.2(0.24)
2	3.3(7.2)	1.2(5)	1(2.3)	15.2(5.9)	13.5(2.9)	5.1(1)	40.2(5.5)	39(2.25)	16(1.6)
3	3.9(12)	1.7(7.5)	1.5(4)	22.2(9)	20(4)	14(3.6)	55.5(8.2)	48(3.8)	24(3)
4	4.8(23)	2.2(21)	2(7)	30(14)	27.5(5.1)	19(4.4)	59(10.8)	57.5(4)	30.5(4)
5	6.0(29)	4.2(26.6)	3.6(17)	31.5(19.3)	27.5(5.85)	20(5.6)	68.6(18)	66(5)	32.4(4.4)
6	7.2(35)	6.4(31)	4.4(20)	33(32)	28.1(12.4)	23.5(8.4)	70.6(22.5)	68.5(7)	36(6.2)
7	12.5(40.6)	10.3(33.3)	6(29)	33.8(36.5)	28.5(18.6)	24(11)	87(33.8)	85.4(8.1)	42(7.4)
8	14(45.6)	12(39)	6.6(32)	35.2(43)	30.2(24.1)	26(16.3)	92.2(40.9)	88(10)	52(9.4)
9	17(55.6)	15.2(49.6)	6.9(45.3)	37(51.8)	32.6(31.6)	27.1(23.6)	94.8(46.4)	90.2(17)	58.5(12)

Note: (a) 573 K, (b) 773 K, (c) 973 K activation. Values in parentheses represent the benzene to α-methyl styrene ratio.

With activation temperature of the sample, the total conversion of cumene is as follows: 573 K > 773 K > 973 K. The highest activity of the 573 K activated samples can be correlated with the total surface acidity (Table III) which is maximum for 573 K activated samples. The lowest activity in case of 973 K activated samples could be due to the decrease in both the surface acidity and surface area of the samples. It is interesting to note that though the activity decreased with increases in the activation temperature, the selectivity to dehydrogenation product increased. Again this reveals that at higher activation temperature, more Lewis acid sites are formed.

From the Table IX it is found that with the increase in the sulfate content up to 7.5 wt%, the total cumene conversion increases and thereafter decreases. Similar observation was also made in case of phosphated titania samples. Comparing the results with phosphated titania samples, sulfated titania samples give more conversion and selectivity to α-methyl styrene ratio. This means the number as well as strength of Lewis acid sites in case of sulfated titania samples is more than phosphated titania samples.

The catalytic activity of phosphate modified titania has been studied towards the alkylation of aromatic compounds. However, this reaction is not feasible with this catalyst probably may be due to lesser acid strength and sites than sulfated titania samples. From the preliminary study it is found that 7.5 wt% sulfate loaded samples of both the series exhibit highest conversion of benzene to cumene. The highest conversion may be due to its high surface area and higher number of acid sites. So for a detail investigation only 7.5 wt% sulfate loaded samples were used. Alkylation of benzene with isopropanol was studied at various benzene to isopropanol molar ratio with varying temperature in the range 453 to 523 K. Benzene conversion increases with the increase in temperature up to 493 K and thereafter decreases (Fig. 15).

However, the isopropanol conversion increases with the increase in temperature even above 493 K. Fig. 15 indicates that the propene formation is very low within 493 K but above 493 K it suddenly increases. This implies that above 493 K isopropanol directly dehydrates to propene thus decreasing the cumene formation. Benzene to isopropanol molar ratio also plays an important role in deciding the product selectivity (Fig. 16). Particularly, the product selectivity is found to be highest at the benzene to isopropanol molar ratio of 10.

The catalytic behaviour of sulfated titania towards the Friedel-Crafts alkylation reactions was also studied by a series of substituted benzenes (Fig. 17). Interestingly, it was found that the alkylation is highest with benzene and lowest with chlorobenzene. In general, methyl substitution enhances the rate of alkylation reaction. So, with toluene, highest conversion is expected than benzene. However, we found the reverse order; the yield of alkylated product in case of benzene is slightly higher than toluene over the sulfated catalysts. Mostly, the toluene alkylation gives the para substituted product, which may be due to the steric factor, thus prohibiting the ortho substitution. This is because the rate of toluene alkylation seems to be limited in medium-pore catalyst by reagent diffusion inside the

TABLE IX Results of cumene cracking/dehydrogenation (mol%) over SO_4^{2-}/TiO_2 activated at 773 K

	Reaction temperature (K)					
Catalysts	523	573	623	673	723	773
TiO_2	0	0	1.2(0.10)	3.5(0.16)	16.2(0.21)	30.7(0.33)
2.5S/TiO_2	0	1.2(5.0)	5.3(3.2)	15.4(2.1)	28.2(1.8)	58.3(1.2)
5.0S/TiO_2	3.4(20.2)	6.1(18.1)	15.0(16.5)	20.2(14.2)	36.5(11.0)	69.9(9.8)
7.5S/TiO_2	7.8(28.3)	16.5(22.3)	26.3(17.2)	34.4(16.3)	48.2(12.3)	95.6(11.7)
10.0S/TiO_2	6.7(25.5)	15.2(20.1)	22.4(16.3)	30.2(13.8)	43.3(11.2)	92.3(9.8)
7.5S/TiO_2 (H*)	8.2(32.7)	17.3(26.3)	28.8(22.3)	36.5(20.4)	50.5(19.1)	96.2(16.2)
10.0S/TiO_2 (H*)	7.3(28.1)	16.4(23.2)	24.3(18.1)	32.2(17.3)	44.0(13.0)	93.6(12.2)

Note: (H*) indicates H_2SO_4 impregnated samples prepared at pH 7. Values in the parentheses represent the benzene to α-methyl styrene ratio.

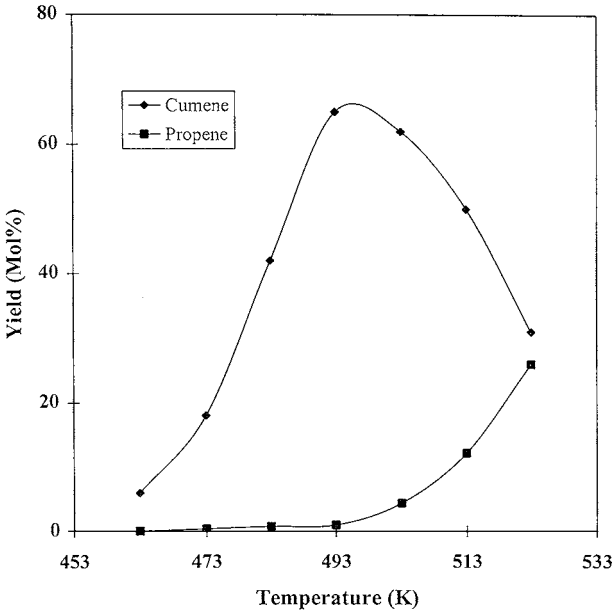

Figure 15 Variation of product selectives of alkylation of benzene with respect to temperature over 7.5S/TiO_2 (H*) at benzene to isopropanol molar ratio of 10.

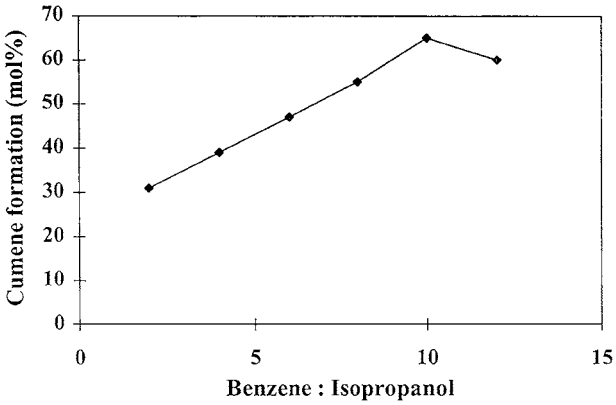

Figure 16 Effect of benzene to isopropanol molar ratio on the cumene formation over 7.5S/TiO_2 (H*) at 493 K.

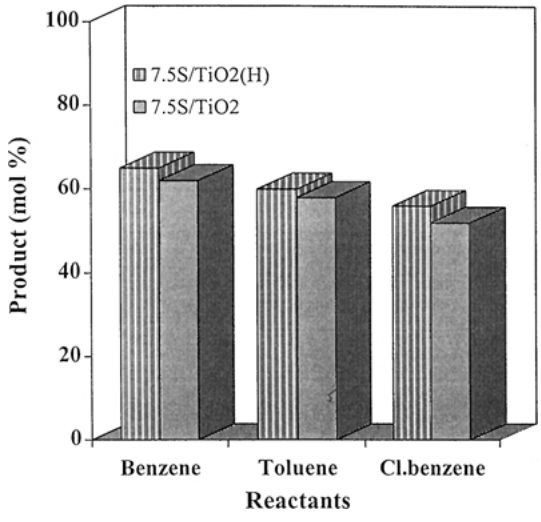

Figure 17 Variation in alkylated product with the variation in reactants over both the SO_4^{-2}/TiO_2 prepared from different methods.

crystal volume. If this is true, the extent of alkylation (% of conversion) will depend on the diffusion coefficient of aromatic hydrocarbon and should follow the order [38].

benzene > toluene > p-xylene > ethylbenzene > m-xylene > o-xylene.

5. Conclusions

1. It is found that phosphate and sulfate impregnation can increase the surface porosity as well as acidity of titania and inhibits sintering at high activation temperatures.

2. However, the surface acid-base sites and the presence of Brönsted and Lewis sites varies with the variation in the method of preparation, source and concentration of phosphate ion.

3. Samples prepared at pH 3 exhibits higher surface area and acid sites, but lower porosity, basic sites and redox sites compared to the sample prepared at pH 7.

4. In the alkylation of benzene with isopropanol, sulfated titania prepared from sulfuric acid showed better activity and selectivity over titania modified with ammonium sulfate.

5. The decrease in the yield of alkyl-substituted benzene above 493 K is the consequence of the preferential dehydration of isopropanol over alkylation reaction.

6. Catalytic proficiency was found to be dependent on sulfate ion concentration in the catalyst, and on the benzene to alcohol molar ration.

Acknowledgments

The authors are thankful to Dr. V.N. Misra, Director, Regional Research Laboratory (CSIR), Bhubaneswar, for his permission to publish this paper. One of the authors, SKS, is obliged to CSIR, Government of India, for senior research fellowship.

References

1. T. JIN, T. YAMAGUCHI and K. TANABE, *J. Phys. Chem.* **90** (1986) 4794.
2. R. A. RAJADHYAKSHA and D. D. CHAUDHARI, *Ind. Eng. Chem. Res.* **26** (1987) 1743.
3. K. ARATA and M. HINO, in Proc. 9th Int. Congr. On Catalysis, edited by M. J. Phillips and M. Ternan (The Chemical Institute of Canada, Ottawa, 1988) Vol. 4, p. 1727.
4. O. SAUR, M. BENSITEL, A. B. MOHAMMED SAAD, J. C. LAVALLEY, C. P. TRIPP and B. A. MORROW, *J. Catal.* **99** (1986) 104.
5. J. CARNEJO, J. STEINLE and H. P. BOEHM, *Z. Naturforsch.* **33B** (1978) 1311.
6. W. W. SWANSON, B. J. STEUSAND and G. A. TSIGDINOS, in Proc. IVth Climax Int. Conf. On Chemistry and Uses of Molybdenum (Ann Arbor, 1982) p. 323.
7. J. HABER, in Proc. VIIIth Int. Congr. Catalysis (Verlag Chemie, Berlin, 1984) Vol. I, p. 85.
8. P. J. GELLINGS, in "Catalysis" Vol. 7, edited by G.C. Bond and G. Webb (Royal Society of Chemistry, London, 1985) p. 105.
9. E. K. JONES, *Adv. Catal.* **8** (1956) 219.
10. E. WEISAND and P. A. ENGELHARD, *Bull. Soc. Chim. Fr.* (1968) 1811.
11. P. FRIENDMAN and K. L. PINDER, *Ind. Eng. Chem. Process. Des. Dev.* **10** (1971) 548.

12. A. HESS and E. KEMNITZ, *Appl. Catal.* A **149** (1997) 373.
13. K. M. PARIDA, M. ACHARYA, S. K. SAMANTARAY and T. MISHRA, *J. Coll. & Interface Sci.* **217** (1999) 388.
14. S. K. SAMANTARAY and K. M. PARIDA, *J. Mol. Catal.* **176** (2001) 151.
15. S. K. SAMANTARAY, T. MISHRA and K. M. PARIDA, *ibid.* **156** (2000) 267.
16. D. J. ROCHFORD, *Aust. J. Mar. Fresh Water Res.* **2** (1951) 1.
17. J. M. CAMPELO, A. GARCIA, J. M. GUTIERREZ, D. LUNA and J. M. MARINA, *J. Coll. & Interface Sci.* **95** (1983) 544.
18. K. KANDORI, S. UCHIDA, S. KATAOKA and T. ISHIKAWA, *J. Mater. Sci.* **27** (1992) 719.
19. D. G. BARTON, S. L. SOLED, G. D. MEITZNER, G. A. FUENTES and E. IGLESIA, *J. Catal.* **181** (1999) 57.
20. L. J. ALEMANY, M. A. LARRUBIA, M. C. JIMENEZ, F. DELGADO and J. M. BLASCO, *React. Kinet. Catal. Lett.* **60**(1) (1997) 41.
21. K. NAKAMOTO, "Infra-Red and Raman Spectra of Inorganic and Coordination Compounds," 4th ed. (Wiley, New York, 1986).
22. G. RAMIS, G. BUSCA, V. LORENZELLI, P. F. ROSSI, M. BENSITEL, O. SAUR and J. C. LAVALLEY, in Proceedings of the IXth International Congress on Catalysis (Calgary, Canada, 1988) p. 1874.
23. A. MENNOUR, C. ECOLIVET, D. COVNET, J. F. HEMIDY, J. C. LAVALLEY, L. MARIETTE and P. ENGELHARD, *Mater. Chem. Phys.* **19** (1988) 301.
24. J. CRIADO and C. REAL, *J. Chem. Soc. Faraday Trans.* **I 79** (1983) 2765.
25. A. D. WARD and I. E. KO, *J. Catal.* **150** (1994) 18.
26. K. M. PARIDA and P. K. PATTNAYAK, *J. Coll. & Interface Sci.* **182** (1996) 381.
27. S. BRUNAUER, D. W. DEMMING, L. S. DEMMING and F. TELLER, *J. Amer. Chem. Soc.* **62** (1940) 1723.
28. E. P. BARRETT, L. G. JOYNER and P. P. HALONDA, *ibid.* **73** (1951) 373.
29. S. J. GREGG and K. S. W. SING, "Adsorption, Surface Area and Porosity," 2nd ed. (Academic Press, New York, 1982).
30. A. K. DALAI, R. SETHURAMAN, S. P. R. KATIKANENI and R. O. IDEM, *Ind. Eng. Chem. Res.* **37** (1998) 3869.
31. B. H. DAVIS, R. A. KEOGH and R. SRINIVASAN, *Catal Today* **20** (1994) 219.
32. M. HINO and K. ARATA, *J. Chem. Soc. Cem. Commun.* (1979) 1148.
33. J. R. SOHN and H. J. KIM, *J. Catal.* **101** (1986) 428.
34. Y. OKAMOTO and T. IMANAKA, *J. Phys. Chem.* **92** (1988) 7102.
35. J. M. LEWIS and R. A. KYDD, *J. Catal.* **132** (1991) 465.
36. J. NAVARRETTE, T. LOPEZ and R. GOMEZ, *Langmuir* **12** (1996) 4385.
37. G. BUSCA, G. RAMIS, V. LORENZELLI and P. F. ROSSI, *ibid.* **5** (1989) 917.
38. N. V. CHOUDHARY, R. V. JASRA, S. G. T. BHAT and T. S. R. PRASAD RAO, Zeolites: facts, figures, future, in "Stud. Surf. Sci. Catal.," Vol. 49B (Elsevier, Amsterdam, 1989) p. 867.

Received 29 August
and accepted 2 September 2002